










Research Article

Intravitreally Administered Soluble VEGF Receptor-1 Variant Tested as a Potential Gene Therapeutic for Diabetic Retinopathy

Steven Hyun Seung Lee ¹, Joo Yong Lee ^{2,3}, Im Kyeong Kang,^{4,5} Jun-Sub Choi ¹,
Hee Jong Kim ¹, Jin Kim,¹ Seho Cha ¹, Kyoung Jin Lee ^{3,5}, Ha-Na Woo ^{3,6},
Keerang Park ¹ and Heuiran Lee ^{3,7}

¹CdmoGen Co., Ltd., Cheongju, Republic of Korea

²Department of Ophthalmology, College of Medicine, Asan Medical Center, University of Ulsan, Seoul, Republic of Korea

³Bio-Medical Institute of Technology, College of Medicine, University of Ulsan, Seoul, Republic of Korea

⁴Department of Medical Science, College of Medicine, Asan Medical Institute of Convergence Science and Technology, Asan Medical Center, University of Ulsan, Seoul, Republic of Korea

⁵Department of Microbiology, College of Medicine, University of Ulsan, Seoul, Republic of Korea

⁶Department of Biochemistry & Molecular Biology, College of Medicine, University of Ulsan, Seoul, Republic of Korea

⁷Department of Microbiology, College of Medicine, Asan Medical Center, University of Ulsan, Seoul, Republic of Korea

Correspondence should be addressed to Keerang Park; keerang.park@gmail.com and Heuiran Lee; heuiran@amc.seoul.kr

Received 27 May 2022; Accepted 13 September 2022; Published 13 October 2022

Academic Editor: Dao Pan

Copyright © 2022 Steven Hyun Seung Lee et al. This is an open access article distributed under the Creative Commons Attribution License, which permits unrestricted use, distribution, and reproduction in any medium, provided the original work is properly cited.

In addition to laser photocoagulation, currently used therapeutic interventions for diabetic retinopathy (DR) include relatively short-lived anti-VEGF drugs targeting vascular endothelial growth factor (VEGF). The latter requires frequent administration via intravitreal injections to effect long-term VEGF suppression. However, due to the patient burden associated with this treatment modality, gene therapy may represent a preferable alternative, providing long-lasting yet patient-friendly effects. Here, we explore the therapeutic efficacy of rAAV2-sVEGFRv-1, a recombinant adeno-associated virus encoding a soluble variant of VEGF receptor-1, upon early DR processes. Bevacizumab, an anti-VEGF agent often prescribed off label to treat DR, was used as an experimental comparator. Administered by intravitreal injection to a streptozotocin-induced diabetic mouse model, rAAV2-sVEGFRv-1 was shown to effectively transduce the mouse retinas and express its transgene therein, leading to significant reductions in pericyte loss and retinal cell layer thinning, two processes that play major roles in DR progression. Acellular capillary formation, vascular permeability, and apoptotic activity, the latter being the cell death mechanism by which retinal neurodegeneration occurs, were also shown to be reduced by the therapeutic virus vector. Immunohistochemistry was used to visualize that rAAV2-sVEGFRv-1 has an effect on cell types important to DR pathophysiology, particularly the ganglion cell layer and glial cells. Combined with our previous work showing that the therapeutic virus vector reduces neovascularization, our current results reveal that rAAV2-sVEGFRv-1 addresses the early aspects of DR as well, thereby demonstrating its potential as a human gene therapeutic versus the condition as a whole.

1. Introduction

Diabetic retinopathy (DR) is a commonly occurring complication of diabetes mellitus (DM) and ranks among the leading causes of blindness worldwide [1]. A degenerative condition presents at pathogenesis as nonproliferative diabetic retinopathy (NPDR) before progressing to proliferative

diabetic retinopathy (PDR), the form of the disease more closely associated with irreversible vision loss. PDR is characterized by neovascularization (NV), a process driven by vascular endothelial growth factor (VEGF), an angiogenic factor whose expression is upregulated in the diabetic retina [2]. As an estimated one quarter [1] of the 592 million DM patients projected by 2035 [3] are predicted to develop DR

to sight-threatening levels, it can be seen that DR is a looming global health concern.

Increased VEGF secretion occurs during DR as a result of the hypoxic retinal environment that develops due to DM-associated hyperglycemia [4]. Among the binding targets of VEGF are two fms-like tyrosine kinase receptors, Flt-1 [5], and KDR/Flk-1 [6], with the interaction with the latter being responsible for driving the angiogenic process. VEGF is additionally implicated in the development of diabetic macular edema (DME), a complication of DR that can occur during either NPDR or PDR [3]. A swelling or thickening of the macula, DME is the most common source of DR-related blindness [7]. Due to the central role of VEGF in the pathology of PDR and DME, which directly threaten the vision of DR patients, the standard of care for both conditions includes anti-VEGF therapeutics [3], as well as laser photocoagulation [4]. Multiple safety and efficacy issues exist for the latter, including complications that contribute to DR progression [8], whereas the former possesses significant limitations inherent to the treatments themselves [9].

Generally, anti-VEGF therapeutics consist of protein-based drugs that are delivered intravitreally [3] and include bevacizumab, a monoclonal antibody commonly utilized off-label for DR due to the significant economic benefits it offers; ranibizumab, a Fab fragment; and aflibercept, a recombinant fusion protein [1, 7, 10]. Comparative studies and meta-analyses have demonstrated that the treatment efficacies of these drugs are not significantly dissimilar [11–13], with the exception of aflibercept for more severe manifestations of the disease. Where advances have been made, however, can be seen in the increased intervals between treatments for the dosing schedule of each successive drug. This is because frequent administration of these relatively short-lived therapeutics is required for long-term VEGF suppression [3, 4], made necessary by the progressive [2] and degenerative nature of DR [4]. However, this may be both procedurally and economically burdensome to the patients, negatively affecting compliance and treatment outcomes. Alternative dosing schedules, such as treat and extend and pro re nata, are currently being explored for these therapeutics to further lengthen treatment intervals, particularly for DME, without significant reductions in efficacy [10]. Yet even these extended schedules require multiple intravitreal injections per year, meaning that a treatment strategy providing anti-VEGF activity in a long-lasting and patient-friendly manner, for which gene therapy is ideally suited, may prove to be highly advantageous.

The therapeutic virus vector rAAV2-sVEGFRv-1 is a recombinant adeno-associated virus 2 (rAAV2) encoding a truncated form (sVEGFRv-1) of sFLT-1, a naturally occurring, alternatively spliced soluble variant of Flt-1 lacking the transmembrane domain found in the full-length VEGF receptor [14]. Nonpathogenic in nature and capable of transducing dividing and nondividing cells to elicit long-term transgene expression [15], rAAV2 vectors are particularly well-suited for delivering gene therapeutics targeting ocular conditions, as exhibited by the regulatory approval of voretigene neparvovec-rzyl, a treatment for Leber's congenital amaurosis type 2 [16]. sFLT-1 has a

high affinity towards VEGF and sequesters it from interacting with KDR/Flk-1 [14], which provides antiangiogenic activity, while also being able to directly associate with KDR/Flk-1, resulting in the formation of inactive heterodimers [17]. As a result, sFLT-1 is able to exert anti-VEGF effects via multiple mechanisms. The antiangiogenic activity of rAAV2-sVEGFRv-1 could be seen in our previous work [18], where it was demonstrated in a laser-induced mouse model of choroidal NV, among other effects.

Here, the therapeutic efficacy of rAAV2-sVEGFRv-1 was tested in comparison to bevacizumab in a streptozotocin (STZ-) induced diabetic mouse model recapitulating the early processes of DR. After in vitro characterization of the therapeutic virus vector was conducted using human umbilical vein endothelial cells (HUVECs), rAAV2-sVEGFRv-1 was administered to the mice via intravitreal injection. There, it was shown to effectively transduce the mouse retinas and therein reduce pericyte loss, acellular capillary formation, vascular leakage, and the thinning of retinal cell layers while also having an antiapoptotic effect. Generally, the therapeutic virus vector compared favorably to bevacizumab, especially in its ability to reduce pericyte loss, an important early contributor to DR progression. Overall, our results show that rAAV2-sVEGFRv-1 demonstrates great promise as a potential human gene therapeutic for the treatment of DR.

2. Materials and Methods

2.1. Virus Vector Development. rAAV2-sVEGFRv-1 and rAAV2-GFP were prepared as previously described [18]. Briefly, the region spanning nucleotide positions 282 to 2,253 of the mRNA for human VEGF receptor-1 (XM_017020485.1; NCBI Reference Sequence, NIH) was inserted into a rAAV2 vector under the control of a CMV promoter along with a SV40 polyadenylation signal and both ITRs to produce rAAV2-sVEGFRv-1. rAAV2-GFP was generated as a negative control by an analogous insertion of an EGFP expression cassette. All virus vectors used in this study were sourced from Cdmogen Co., Ltd. (Cheongju, Korea).

2.2. Cell Culture and Infection. HUVECs (Lonza, Basel, Switzerland) were maintained in EGM-2 (Lonza) supplemented with EGM-2 Single Quots (Lonza). Cells were infected with their respective virus vectors at an MOI of 10,000.

2.3. Real-Time PCR. Total RNA was extracted from infected HUVECs using TRIzol (Thermo Fisher Scientific, Waltham, MA), per the manufacturer's instructions, and the total RNA treated with DNase I (Thermo Fisher Scientific) to eliminate contamination by viral genomic DNA. cDNA was synthesized using M-MLV reverse transcriptase (Elpis Biotech, Daejeon, Korea) and real-time PCR performed using primers for the Flt-1 and β -actin genes, as follows: Flt-1 F: CGTGTAAAGGAGTGGACCATC, Flt-1 R: TAAGACCGC TTGCCAGCTAC, β -actin F: TGAAGATCAAGATCAT TGCTC, and β -actin R: TGCTTGCTGATCCACATCTG.

2.4. Tube Formation Assay. Control and rAAV2-sVEGFRv-1-infected HUVECs were seeded in a 96-well μ -plate (Ibidi,

Gräfelfing, Germany) at 20,000 cells/well and the manufacturer's protocol followed for the tube formation assay. VEGF treatment was performed using Recombinant Human VEGF 165 Protein (293-VE-050; R&D Systems, Minneapolis, MN) at a concentration of 10 ng/mL and preincubated with conditioned media for 30 minutes. Five hours post cell seeding, results were obtained, and the percentage of tube areas was calculated using ImageJ (National Institutes of Health, Bethesda, MD).

2.5. Animal Care. All animal care and experiments were overseen by the Internal Review Board for Animal Experiments at the Asan Institute for Life Sciences (University of Ulsan, College of Medicine) and performed in accordance with the Association for Research in Vision and Ophthalmology Resolution on the Use of Animals in Ophthalmic and Vision Research. Mice were housed in cages containing 5 animals apiece in the same area of a 25°C temperature-controlled room with free access to water and chow and an alternating photoperiod of 12 hours of light and dark.

2.6. STZ-Induced Diabetic Mouse Model. A well-established protocol [19] for inducing diabetes mellitus in mice via the administration of a single high dose of STZ was followed using 7-week-old male C57/BL6 mice sourced from the Orient Bio (Sungnam, Korea), with minor modifications. To mitigate the possibility of death due to STZ-induced toxicity, mice were injected intraperitoneally with 150 mg/kg of STZ (Sigma-Aldrich, St. Louis, MO), rather than the 200 mg/kg specified. Additionally, 10% sucrose water was provided only to mice that experienced significant deterioration, determined via reductions in body weight (Supplementary Table 1). Successful generation of the diabetic model was confirmed in mice whose tail vein blood samples, taken 1 week post-STZ treatment, had blood glucose levels exceeding 300 mg/dL (Supplementary Table 2), measured using Accu-Chek (Roche Diagnostics, Indianapolis, IN).

2.7. Intravitreal Injections. Mice were anesthetized 1 month post-STZ treatment via intraperitoneal injection of a 4:1 mixture of 40 mg/kg Zoletil (zolazepam/tiletamine) from Virbac (Carros Cedex, France) and 5 mg/kg of Rompun (xylazine) from Bayer Healthcare (Leverkusen, Germany). The pupils were dilated with Mydrin-P (0.5% tropicamide and 2.5% phenylephrine) from Santen (Osaka, Japan), and then, both eyes were injected intravitreally with 1 μ L of either rAAV2-sVEGFRv-1 or rAAV2-GFP at a concentration of 5.0×10^{10} viral genomes (v.g.)/mL. Bevacizumab was administered to anesthetized mice at 25 mg/kg.

2.8. Sacrifice and Tissue Preparation. Sacrifice occurred at either 2 or 5 months post intravitreal injection. Mice were deeply anesthetized using a 4:1 mixture of Zoletil (80 mg/kg) and Rompun (10 mg/kg), after which intracardial perfusion with 0.1 M PBS (7.4 pH) containing 150 U/mL heparin and infusion with 4% paraformaldehyde (PFA) in 0.1 M phosphate buffer (PB) were performed. To generate eyecups, the eyeballs were enucleated and fixed in 4% PFA in 0.1 M PB for 1 hour, and the anterior sections were removed, including the cornea and lens, before being placed overnight

in 30% sucrose in PBS. Prior to preparing 5-10 μ m thick frozen transverse retinal sections, eyecups were embedded in Tissue-Tek (Miles Scientific, Naperville, IL), an optimal cutting temperature compound.

2.9. ELISA. To determine human sVEGFRv-1 concentrations in vitro and in vivo, culture media were collected from infected HUVECs and vitreous humor sampled 10 days after the intravitreal injection of rAAV2-sVEGFRv-1, respectively. ELISA was then performed using the Human VEGFR1/Flt-1 Quantikine ELISA Kit (DVRI00C; R&D Systems), according to the manufacturer's protocol.

2.10. Immunohistochemistry. An antibody for human VEGFR1/Flt-1 (AF321; R&D Systems) was used to immunostain section samples, and anti-NeuN (MAB377; Millipore, Burlington, MA) and anti-GFAP (12389; Cell Signaling Technology, Danvers, MA) were used to visualize retinal cells. The samples were incubated overnight with diluted primary antibodies at 4°C, followed by washing in PBST 3 times for 10 minutes apiece, incubation for 2 hours with the secondary antibodies Alexa Fluor 568 or 488 (Thermo Fisher Scientific) at room temperature, and staining with DAPI (D9542; Sigma-Aldrich). A LSM 710 fluorescence confocal microscope (Carl Zeiss Microscopy, Jena, Germany) was used to examine the section samples, and images were captured using the black edition of the Zeiss Zen software (Carl Zeiss Microscopy), followed by analysis using ImageJ.

2.11. Retinal Trypsin Digest. To observe the retinal vasculature, enucleated eyeballs were fixed for 24 hours in 10% formalin solution and washed in PBS before the retina was isolated and trypsin digestion performed [20], with minor modifications to the protocol. The retina was incubated in a 3% trypsin solution (15090046; Thermo Fisher Scientific) in 0.1 M Tris buffer (pH 7.8) for 1 hour at 37°C with gentle shaking, washed with water, and stained using conventional hematoxylin and eosin (H&E) methods. Light microscopy was used to determine the numbers of retinal pericytes and acellular capillaries in the center of the retinal area, with the former identified via its morphology (bound to capillaries and rounded nuclei). The number of pericytes and acellular capillaries was counted in 5 randomly selected 1 mm \times 1 mm areas of the retinal capillaries, standardized using the retinas of normal control mice, and the data were expressed as a ratio.

2.12. FITC-Dextran Staining. Vascular leakage was visualized via tail vein injection of 50 mg/mL of FITC-dextran (FD2000S; Sigma-Aldrich) 30 minutes prior to sacrifice and the fixing of enucleated eyeballs for 1 hour in 10% formalin solution. After washing with PBS, the retinas were isolated from the RPE-choroid complex and flat mounts generated via four equidistant cuts prior to observation via fluorescence microscopy (Eclipse Ti-U; Nikon, Tokyo, Japan), with the detailed images taken at 100x magnification.

2.13. Determination of Retinal Cell Layer Thinning. Frozen transverse sections, including the optic nerve head, were

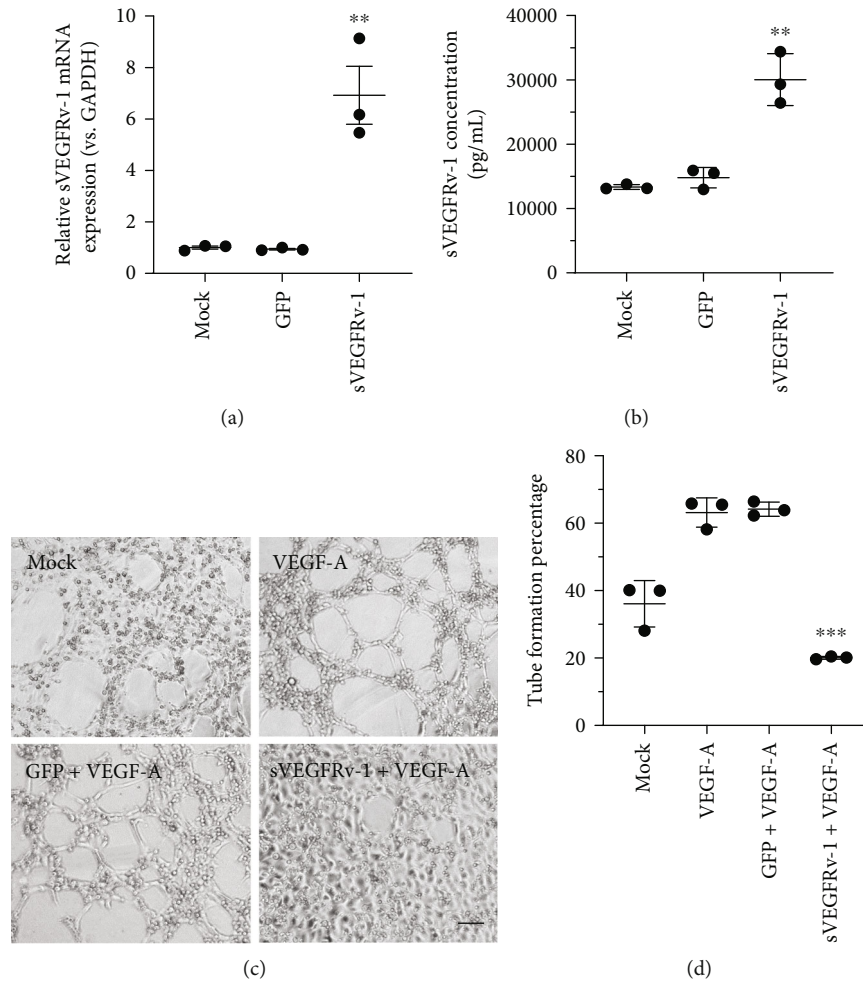


FIGURE 1: Characteristics of rAAV2-sVEGFRv-1. In vitro characterization was performed using HUVECs, which showed via real-time PCR ($n = 3$) (a) and ELISA ($n = 3$) (b) that rAAV2-sVEGFRv-1 treatment led to significant increases in the mRNA and expression levels of the soluble VEGF receptor-1 variant, respectively, compared to mock-infected control cells and those infected with a virus vector expressing GFP. A tube formation assay showed (c) that the therapeutic virus vector markedly reduced (d) the formation of tube-like structures preceding VEGF-driven neovascularization ($n = 3$). ** $p < 0.01$ and *** $p < 0.001$.

stained using H&E methods, and the cell layers were visualized using ImageJ). By determining, as a ratio, the changes of the inner retina from the nerve fiber layer to the inner nuclear layer, the extent of retinal cell layer thinning was calculated using the following equation: [mean (ratio of inner retina) = (thickness from nerve fiber layer to inner nuclear layer)/(thickness from nerve fiber layer to outer nuclear layer)].

2.14. TUNEL Assay. TUNEL assay (12156792910; Roche Diagnostics) was performed following the manufacturer's instructions, and the frozen sections were washed in PBST 3 times for 10 minutes apiece before being stained with DAPI to visualize the cell nuclei.

2.15. Statistical Analysis. Statistical analysis was performed using paired T -testing, with significant difference determined versus sham at ** $p < 0.01$ or *** $p < 0.001$, whereas significant difference versus bevacizumab was signified using

double crosses (†† $p < 0.01$). Data was visualized using dot plot graphs and includes significance and mean standard error of mean values.

3. Results

3.1. rAAV2-sVEGFRv-1 Is Able to Effectively Infect Endothelial Cells as well as Transduce Mouse Retinas to Express Its Transgene. 72 hours post infection, total RNA and culture media were collected from infected HUVECs in order to determine the in vitro characteristics of the therapeutic virus vector. Real-time PCR (Figure 1(a)) showed that relative to uninfected control cells (1.000 ± 0.940), rAAV2-sVEGFRv-1 infection led to an increase in sVEGFRv-1 mRNA levels (6.920 ± 1.960) while rAAV2-GFP treatment did not (0.940 ± 0.060), with a similar pattern of results obtained by ELISA (Figure 1(b)). The activity of the expressed sVEGFRv-1 was then examined via tube formation assay (Figure 1(c)), as endothelial cells under

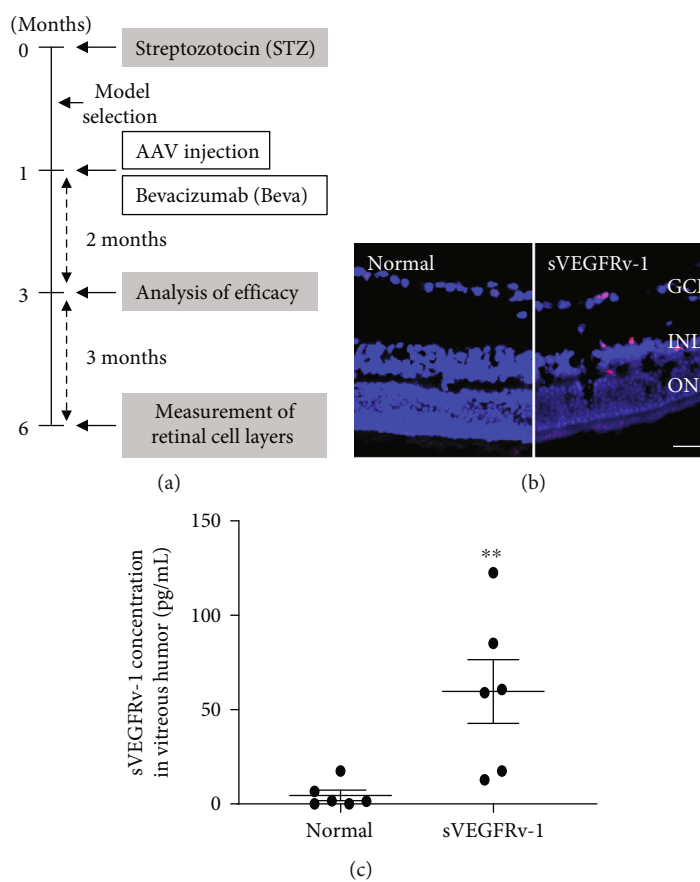


FIGURE 2: Animal experimental design and the in vivo efficacy of rAAV2-sVEGFRv-1. Experimental schematic (a). Immunohistochemistry performed on transverse section samples demonstrated human sVEGFRv-1 expression (red) in the retinas of the STZ-induced diabetic mouse model two months post intravitreal injection (b). Concentration of sVEGFRv-1 secreted into the vitreous humor as a result of effective retinal transduction was quantified by ELISA ($n = 6$) with the vitreous humor sampled 10 days after rAAV2-sVEGFRv-1 administration (c). Scale bar: $50 \mu\text{m}$; ** $p < 0.01$.

VEGF stimulation form tube-like structures prior to the development of NV [21]. Compared to uninfected and untreated control HUVECs (36.080 ± 6.886), tube formation was significantly elevated in VEGF-stimulated cells infected with rAAV2-GFP (64.171 ± 2.109), as well as uninfected HUVECs treated with VEGF (63.159 ± 4.343). On the other hand, cells stimulated with VEGF and infected with rAAV2-sVEGFRv-1 (20.076 ± 0.415) exhibited levels of tube formation that were below even that of the control cells (Figure 1(d)).

Having thus examined the in vitro efficacy of rAAV2-sVEGFRv-1, an STZ-induced diabetic mouse model was established (Figure 2(a)) to explore the in vivo effects of the therapeutic virus vector. Retinal transduction was shown to occur from a single intravitreal administration of rAAV2-sVEGFRv-1 and was visualized by immunostaining transverse section samples with an antibody for the secreted sVEGFRv-1 (Figure 2(b)). ELISA showed that sVEGFRv-1 expression was significantly elevated (Figure 2(c)) in mice injected with rAAV2-sVEGFRv-1 ($59.600 \pm 41.400 \text{ pg/mL}$) when compared to the normal control group ($4.500 \pm 6.700 \text{ pg/mL}$).

3.2. rAAV2-sVEGFRv-1 Reduces Pericyte Loss, the Formation of Acellular Capillaries, and Leaky Vessel Development. Relative to normal control mice (1.000 ± 0.082), rAAV2-sVEGFRv-1 administration resulted in a marked reduction in the loss of pericytes (0.740 ± 0.080), which is among the earliest observed manifestations of DR [7] and demonstrated here via trypsin digestion assay (Figure 3(a), white arrowheads). The extent of this reduction, measured 3 months after establishing the model system and 2 months post intravitreal injection (Figure 3(b)), was greater than of mice treated with bevacizumab (0.480 ± 0.050), whereas pericyte loss readily occurred in both control rAAV2-GFP-treated mice (0.300 ± 0.055) and the STZ-induced diabetic mouse model (0.280 ± 0.062).

Among other effects, pericyte loss may lead to retinal nonperfusion [7, 22], which may be observed in diabetic animal models in the form of acellular capillaries [22]. Acellular capillary formation (Figure 3(a), black arrows) was virtually absent in the normal control group (0.600 ± 0.548) while being elevated in mice injected with the control virus vector (9.400 ± 1.673) and the sham-treated diabetic mouse model (9.800 ± 1.924). In contrast, treatment with the therapeutic

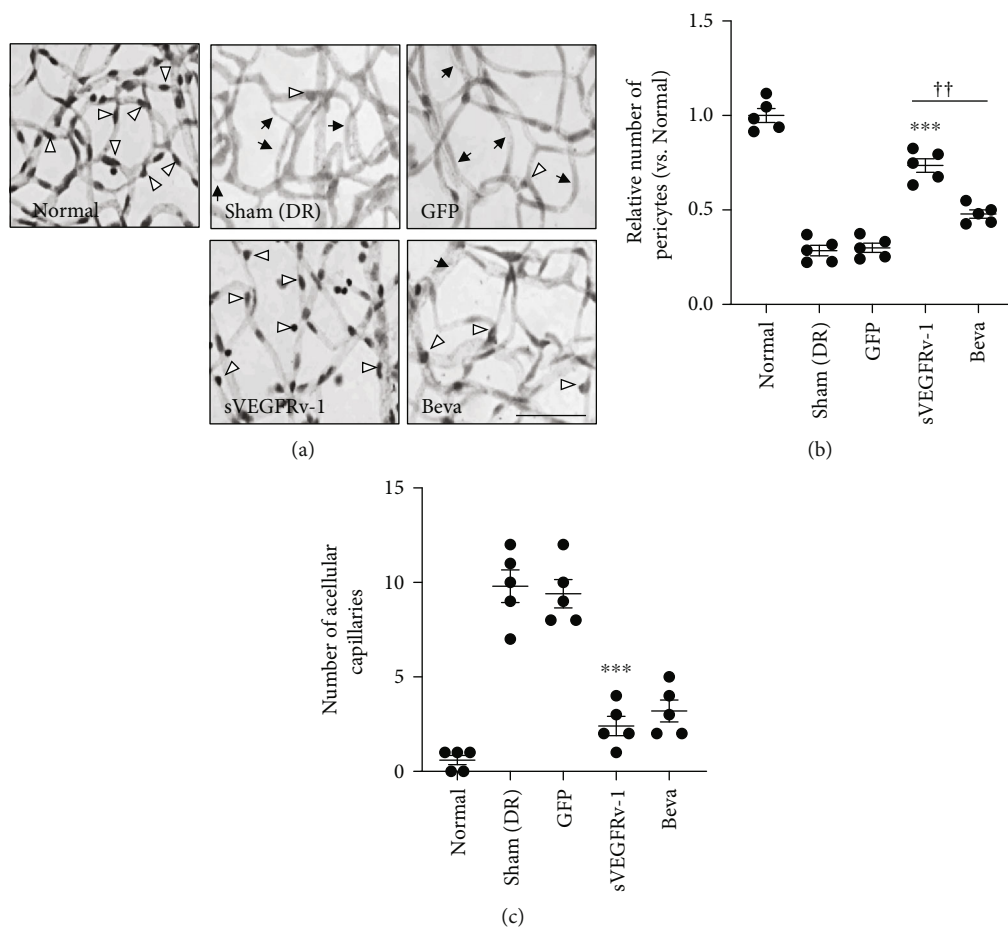


FIGURE 3: rAAV2-sVEGFRv-1 reduces retinal pericyte loss, acellular capillary formation, and vascular leakage. rAAV2-sVEGFRv-1 was shown to reduce retinal pericyte loss, which is linked to the formation of acellular capillaries, indicated in the retinal vascular histology by white arrowheads and black arrows, respectively (a). In order to highlight its particular efficacy in reducing pericyte loss, this effect of rAAV2-sVEGFRv-1 was additionally compared to bevacizumab ($n = 5$) (b). The same quantification, however, was not performed in the acellular capillary formation statistical analysis ($n = 5$) (c). Scale bar: $100 \mu\text{m}$; *** $p < 0.001$ vs. sham; †† $p < 0.01$ vs. bevacizumab.

virus vector (2.400 ± 1.140) and bevacizumab (3.200 ± 1.304) both reduced the formation of these structures, with this effect being more pronounced in mice injected with rAAV2-sVEGFRv-1 (Figure 3(c)).

In turn, retinal nonperfusion is linked to the development of retinal vasodegeneration and the subsequent formation of vascular leakage, another key feature of the earlier stages of DR [23] and a process that may result in DR-related vision loss. Leaky vessels were visualized 2 months post intravitreal injection via FITC-dextran staining of retinal flat mounts (Figure 4(a)). In normalized to untreated control mice (1.000 ± 0.142), vascular leakage was observed in the sham- (1.944 ± 0.193) and rAAV2-GFP-treated (1.925 ± 0.200) control groups, but this process was significantly reduced when rAAV2-sVEGFRv-1 (1.105 ± 0.119) and bevacizumab (1.168 ± 0.094) were administered (Figure 4(b)).

3.3. Decreased Retinal Cell Layer Thinning and Antiapoptotic Activity Suggest That rAAV2-sVEGFRv-1 Is Neuroprotective.

In addition to pericytes, other vascular and neuronal cells of

the retina are involved in DR progression [2, 24], and H&E staining was used to visualize the thinning of the retinal cell layers (Figure 5(a)). Relative to normal control mice (1.000 ± 0.088), cell layer thinning was observed in the diabetic mouse model (0.729 ± 0.088) and the rAAV2-GFP-treated control group (0.747 ± 0.076). However, this process was markedly reduced (Figure 5(b)) by rAAV2-sVEGFRv-1 treatment (0.931 ± 0.040), with this effect being especially pronounced in the inner nuclear layer, suggesting that the therapeutic virus vector may have neuroprotective qualities. However, comparisons to bevacizumab were not made here, as retinal cell layer thinning was determined 5 months post intravitreal injection in order to examine the long-lasting effects of rAAV2-sVEGFRv-1.

Meanwhile, a TUNEL assay performed 2 months after virus vector treatment showed that apoptotic cells were almost wholly absent (Figure 6(a)) in normal control mice (0.400 ± 0.548), whereas TUNEL-positive cells were found speckled throughout the retinal cell layers of the STZ-induced diabetic mouse model (9.600 ± 1.517) and mice treated with rAAV2-GFP (10.600 ± 2.408). On the other

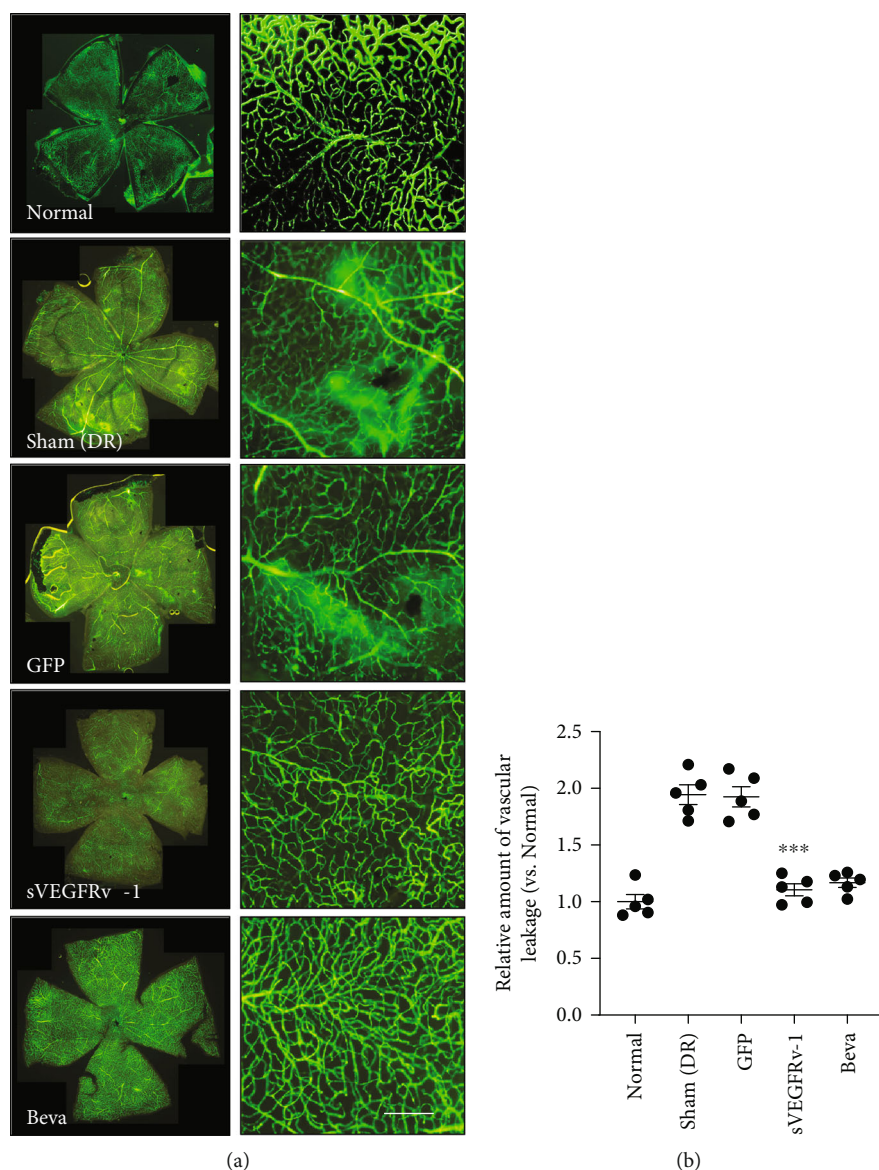


FIGURE 4: Retinal vascular permeability is reduced by rAAV2-sVEGFRv-1. Linked to retinal vasodegeneration and the subsequent development of DR-related vision loss, vascular leakage is observable in retinal flat mounts (a, left column) as blurred regions of FITC-dextran staining, with the details becoming more distinguishable at 100x magnification (a, right column). The quantification of leaky vessel formation was determined ($n = 5$) as a ratio relative to normal control mice (b). Scale bar: $50 \mu\text{m}$; *** $p < 0.001$ vs. sham.

hand, the administration of rAAV2-sVEGFRv-1 (2.200 ± 1.304) and bevacizumab (3.800 ± 2.387) both resulted in a reduction in observed apoptotic activity (Figure 6(b)).

3.4. rAAV2-sVEGFRv-1 Protects against Glial Cell Activation and the Loss of Ganglion Cells in Diabetic Mouse Retinas.

The effects of rAAV2-sVEGFRv-1 upon the diabetic retina were additionally visualized using anti-NeuN (Figure 7(a)) and anti-GFAP (Figure 7(b)), which stain ganglion cells and glial cells, respectively. While NeuN-positive cells were found in both sham-treated mice (5.400 ± 1.673) and those injected with the control virus vector (4.200 ± 1.643), the greatest number was observed (Figure 7(c)) in the retinas of mice treated with rAAV2-sVEGFRv-1 (14.200 ± 1.924),

bevacizumab (11.400 ± 1.673), or the normal control group (12.800 ± 1.643).

Conversely, GFAP expression was elevated in rAAV2-GFP-treated mice (1.062 ± 0.107) and the sham-treated diabetic mouse model (1.000 ± 0.203), indicating higher amounts of active glial cells. Relative to the latter, GFAP expression was markedly reduced (Figure 7(d)) in mice injected with bevacizumab (0.452 ± 0.100) and rAAV2-sVEGFRv-1 (0.409 ± 0.123), as well as normal control mice (0.326 ± 0.147).

4. Discussion

Due to the limitations of laser photocoagulation and/or anti-VEGF therapeutics, currently the most commonly employed

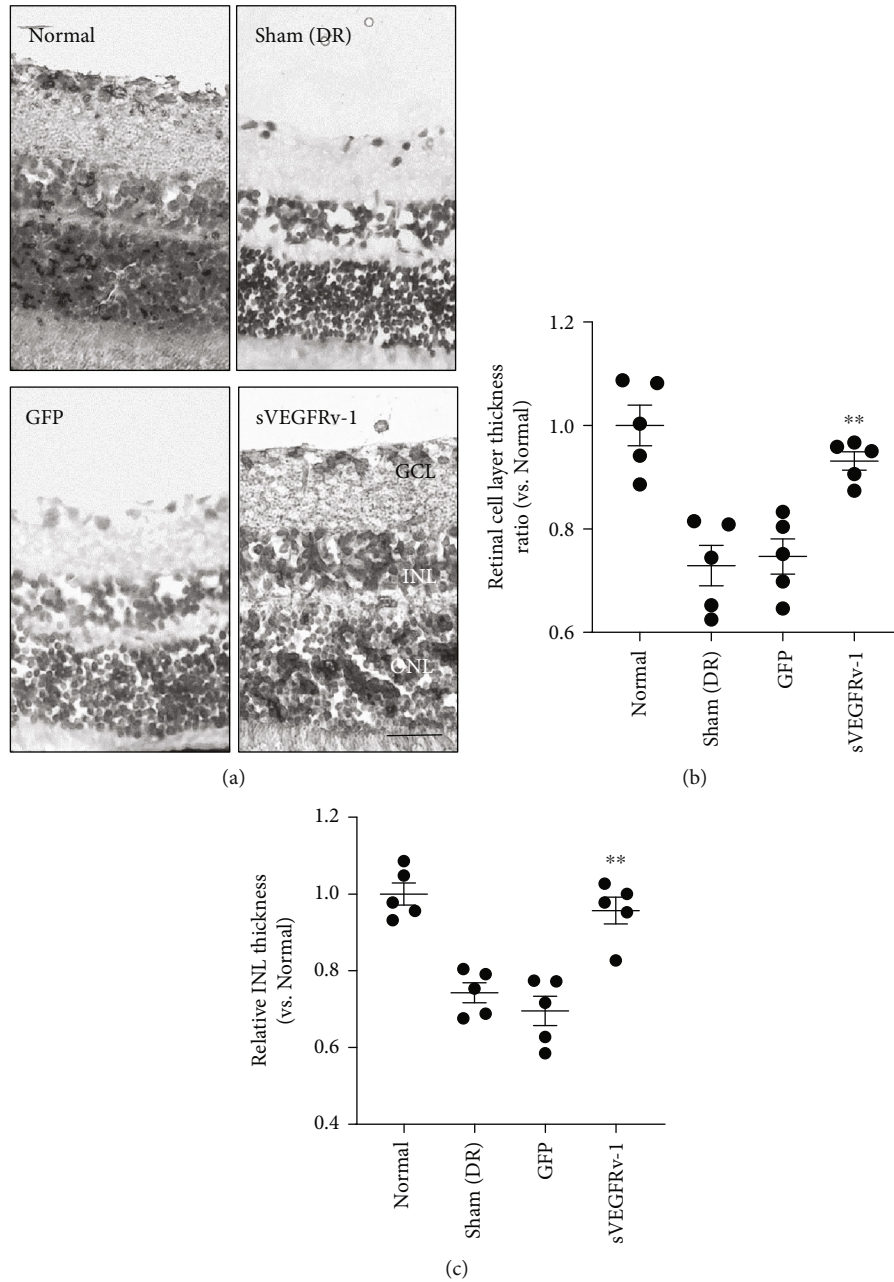


FIGURE 5: rAAV2-sVEGFRv-1 protects against retinal cell layer thinning. The effect of the therapeutic virus vector upon the cell layers of the mouse retinas suggests that rAAV2-sVEGFRv-1 has neuroprotective qualities. This can be seen in the changing thicknesses of the retinal cell layers (a), visualized 5 months post intravitreal injection and calculated as a ratio relative to normal control mice ($n = 5$) (b), with the effect on the inner nuclear layer being noted specifically ($n = 5$) (c). Scale bar: $50 \mu\text{m}$; $**p < 0.01$ vs. sham.

treatment options for DR and DME, the development of a gene therapy alternative [25] may provide the answer in effecting safe and long-term VEGF suppression while reducing patient burden. Laser-based treatment, in the form of panretinal photocoagulation, has been linked to the formation of subretinal fibrosis [26], vascular leakage, and choroidal NV [8], all of which are implicated in DR pathoprogression, whereas anti-VEGF DR drugs, in addition to risks associated with the injection procedure [4], are short-lived while requiring multiple loading injections to begin exerting a therapeutic effect [27]. Yet despite newer

DR therapeutics continuing to be and having been developed and approved, directly targeting VEGF remains unchanged as the treatment strategy.

As such, we initially explored the therapeutic potential of intravitreally injected rAAV2-sVEGFRv-1, its antiangiogenic activity in particular, in a laser-induced mouse model of choroidal NV, an animal model system for the wet subtype of age-related macular degeneration (wAMD) [18]. There, it was shown to reduce the extent to which choroidal NV occurred at levels comparable to bevacizumab, in addition to being antiapoptotic and reducing inflammatory cell

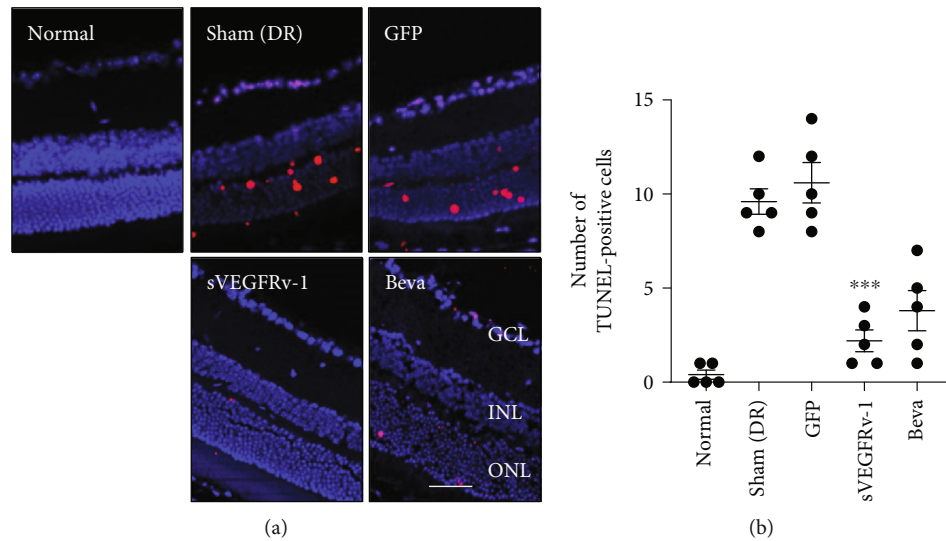


FIGURE 6: Antiapoptotic effect of rAAV2-sVEGFRv-1. TUNEL staining (a) demonstrated that apoptotic cells were readily observed in mock- and rAAV2-GFP-treated mice, while generally being absent in mice administered bevacizumab and the therapeutic virus vector ($n = 5$) (b). Scale bar: $50 \mu\text{m}$; *** $p < 0.001$ vs. sham.

infiltration. The relevance of this study can be linked to the developmental trajectory of anti-VEGF DR drugs, the most common of which were originally used to treat wAMD before being indicated for PDR and DME, as wAMD, like PDR, is characterized by VEGF-driven NV leading to vision loss [10]. A number of these therapeutics subsequently received regulatory approval for all stages of DR [28, 29], and here, we explored the effects of rAAV2-sVEGFRv-1 in a STZ-induced diabetic mouse model. While STZ-induced diabetic mice do not recapitulate the vascular aspects of DR [30], they accurately portray early processes of DR pathophysiology that work to influence disease progression, including the loss of pericytes and resulting retinal vessel dysfunction [31], as well as neurodegeneration [23]. Bevacizumab was used as an experimental comparator in both studies as it was among the most widely used anti-VEGF agents up to the very recent past [10].

As a key histopathological characteristic of DR [32], pericyte loss is linked to the hyperglycemic conditions present in the diabetic retina and is observed early on in the pathophysiology of DR [7]. Due to the important role played by pericytes in normal retinal function [32], their loss is an influential factor in DR pathophysiology [22]. With pericytes playing a crucial role in maintaining the structural integrity of retinal vessels [22], their loss may lead to other vessel abnormalities, including capillary occlusion, ischemia [7], and/or nonperfusion [22]. As a result, the retinal environment may become hypoxic, leading to hypoxia inducible factor 1 (HIF-1) activation and the upregulation of its downstream target, VEGF [7]. In addition to its role driving NV during PDR, VEGF contributes to DR progression in the early stages of the condition [33]. Pericyte loss and VEGF are also linked to the formation of leaky vessels as a result of retinal vasodilation [22, 34]. This may be due to the role pericytes play in proper tight junction formation [22], as several studies have suggested that VEGF induces conformational changes upon tight junctions [4], leading

to vascular leakage and potential DR-related vision loss. In addition to showing that rAAV2-sVEGFRv-1 has anti-VEGF activity (Figure 1), the therapeutic virus vector was additionally demonstrated here to reduce pericyte loss (Figure 3) and the subsequent development of leaky vessels (Figure 4).

However, retinal pericytes are not the only cell type affected by DR, with the condition also influencing endothelial cells, glial cells, and ganglion cells, which collectively form the neurovascular unit (NVU) [2, 24]. In some respects, DR can be considered a disease of the NVU [2], with NVU neurodegeneration constituting a major component of DR progression [35]. Retinal neurodegeneration is characterized by the loss of various amacrine cells [2] and ganglion cells, inner nerve fiber layer thinning [23], and glial cell activation and dysfunction [36]. By determining the changes to the thickness of the inner retina, which includes the ganglion cell layer and inner nerve fiber layer, rAAV2-sVEGFRv-1 was demonstrated to reduce retinal cell layer thinning (Figure 5) while specifically protecting against the loss of retinal ganglion cells, which are particularly susceptible to neurodegenerative effects [23]. The latter was visualized via anti-NeuN staining, whereas the low levels of GFAP expression resulting from rAAV2-sVEGFRv-1 administration (Figure 7) showed that the therapeutic virus vector reduced glial cell activation and activity [36]. rAAV2-sVEGFRv-1, which previously demonstrated its antiapoptotic activity in a laser-induced mouse model of choroidal NV [18], was confirmed here to suppress apoptosis (Figure 6), an important contributor to DR pathophysiology [35] and the cell death mechanism by which neurodegeneration occurs [32]. Apoptosis has also been implicated in the development of vascular leakage [7, 32]. Taken together, these results strongly suggest that the therapeutic virus vector has neuroprotective qualities, thereby addressing another major contributor to DR pathophysiology and progression.

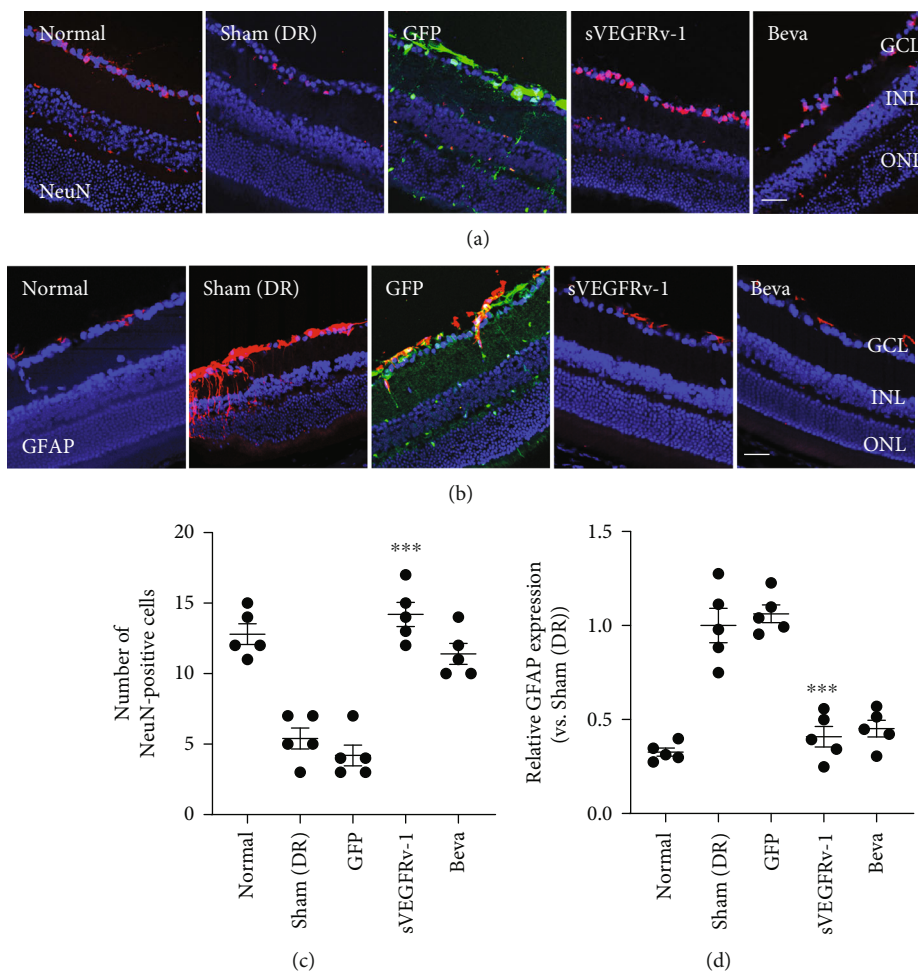


FIGURE 7: rAAV2-sVEGFRv-1 activity in various retinal tissues. Frozen section samples were immunostained with anti-NeuN and anti-GFAP to visualize the ganglion cell layer (a) and glial cells (b), respectively, in the retinas of the STZ-induced mouse model. It was seen that rAAV2-sVEGFRv-1 administration had a preservative effect on retinal ganglion cells ($n = 5$) (c), while leading to a decrease in glial cells ($n = 5$) (d). Scale bar: $50 \mu\text{m}$; *** $p < 0.001$ vs. sham.

5. Conclusions

Therefore, in combination with our previous work demonstrating the antiangiogenic properties of rAAV2-sVEGFRv-1, the ability of the therapeutic virus vector to address early aspects of DR pathophysiology exhibits its great promise as a potential human gene therapeutic versus DR. rAAV2-sVEGFRv-1 generally compared positively to currently used treatments, particularly in reducing pericyte loss, a consequential process in DR progression. Future studies for the continuing development of rAAV2-sVEGFRv-1 as a human gene therapeutic include long-term safety and efficacy studies in nonhuman primates and are currently being planned.

Data Availability

Data is available upon request from the authors.

Conflicts of Interest

S.H.S.L., J.-S.C., H.J.K., J.K., S.C., and K.P. are employees of Cdmogen Co., Ltd., in which S.H.S.L. and K.P. have per-

sonal financial interests. No other potential conflicts of interest relevant to this article were reported.

Authors' Contributions

H.L. and K.P. were responsible for the conceptualization. H.L., J.Y.L., S.H.S.L., I.K.K., H.J.K., J.K., and S.C. were responsible for the methodology. H.L., J.Y.L., S.H.S.L., I.K.K., J.-S.C., H.-N.W., K.J.L., and K.P. were responsible for the investigation. H.L., J.Y.L., S.H.S.L., I.K.K., J.-S.C., and K.P. were responsible for the writing—original draft. H.L., J.Y.L., S.H.S.L., I.K.K., H.-N.W., K.J.L., and K.P. were responsible for the writing—review and editing. Steven Hyun Seung Lee, Joo Yong Lee, and Im Kyeong Kang are co-first authors.

Acknowledgments

We would like to acknowledge S.H.S.L.'s dissertation, "Inhibiting the mechanistic target of rapamycin (mTOR) via RNA interference as a novel human gene therapeutic strategy for the treatment of diabetic retinopathy," which

also discusses the development of a gene therapeutic for diabetic retinopathy. This work was supported by grants from TIPS (Korea Tech Incubator Program for Startup, administered by the Republic of Korea Ministry of SMEs and Startups) to CuroGene Life Sciences Co., Ltd, which was recently acquired by Cdmogen Co., Ltd., and from the National Research Foundation of Korea (NRF-2021R1A2C1093614) to H.L.

Supplementary Materials

Supplementary Table 1: body weights (g) of the STZ-induced diabetic mouse model. Body weight data of the mice from which the STZ-induced diabetic mouse model was generated. Supplementary Table 2: blood glucose levels (mg/dL) of the STZ-induced diabetic mouse model. Blood glucose data of the mice from which the STZ-induced diabetic mouse model was generated. (*Supplementary Materials*)

References

- [1] V. S. Dedania and S. J. Bakri, "Novel pharmacotherapies in diabetic retinopathy," *Middle East African Journal of Ophthalmology*, vol. 22, no. 2, pp. 164–173, 2015.
- [2] A. W. Stitt, N. Lois, R. J. Medina, P. Adamson, and T. M. Curtis, "Advances in our understanding of diabetic retinopathy," *Clinical Science (London, England)*, vol. 125, no. 1, pp. 1–17, 2013.
- [3] E. J. Duh, J. K. Sun, and A. W. Stitt, "Diabetic retinopathy: current understanding, mechanisms, and treatment strategies," *JCI Insight*, vol. 2, no. 14, article e93751, 2017.
- [4] F. Bandello, R. Lattanzio, I. Zucchiatti, and C. Del Turco, "Pathophysiology and treatment of diabetic retinopathy," *Acta Diabetologica*, vol. 50, no. 1, pp. 1–20, 2013.
- [5] C. de Vries, J. A. Escobedo, H. Ueno, K. Houck, N. Ferrara, and L. T. Williams, "The fms-like tyrosine kinase, a receptor for vascular endothelial growth factor," *Science*, vol. 255, no. 5047, pp. 989–991, 1992.
- [6] B. I. Terman, M. Dougher-Vermazen, M. E. Carrion et al., "Identification of the KDR tyrosine kinase as a receptor for vascular endothelial cell growth factor," *Biochemical and Biophysical Research Communications*, vol. 187, no. 3, pp. 1579–1586, 1992.
- [7] W. Wang and A. C. Y. Lo, "Diabetic retinopathy: pathophysiology and treatments," *International Journal of Molecular Sciences*, vol. 19, no. 6, p. 1816, 2018.
- [8] S. V. Reddy and D. Husain, "Panretinal photocoagulation: a review of complications," *Seminars in Ophthalmology*, vol. 33, no. 1, pp. 83–88, 2018.
- [9] L. S. Lim, C. M. G. Cheung, P. Mitchell, and T. Y. Wong, "Emerging evidence concerning systemic safety of anti-VEGF agents - should ophthalmologists be concerned?," *American Journal of Ophthalmology*, vol. 152, no. 3, pp. 329–331, 2011.
- [10] M. W. Stewart, "Extended duration vascular endothelial growth factor inhibition in the eye: failures, successes, and future possibilities," *Pharmaceutics*, vol. 10, no. 1, article E21, 2018.
- [11] The Diabetic Retinopathy Clinical Research Network, "Aflibercept, bevacizumab, or ranibizumab for diabetic macular edema," *The New England Journal of Medicine*, vol. 372, no. 13, pp. 1193–1203, 2015.
- [12] J. A. Wells, A. R. Glassman, A. R. Ayala et al., "Aflibercept, bevacizumab, or ranibizumab for diabetic macular edema: two-year results from a comparative effectiveness randomized clinical trial," *Ophthalmology*, vol. 123, no. 6, pp. 1351–1359, 2016.
- [13] S. B. Bressler, D. Liu, A. R. Glassman et al., "Change in diabetic retinopathy through 2 years: secondary analysis of a randomized clinical trial comparing aflibercept, bevacizumab, and ranibizumab," *JAMA Ophthalmology*, vol. 135, no. 6, pp. 558–568, 2017.
- [14] R. L. Kendall and K. A. Thomas, "Inhibition of vascular endothelial cell growth factor activity by an endogenously encoded soluble receptor," *Proceedings of the National Academy of Sciences*, vol. 90, no. 22, pp. 10705–10709, 1993.
- [15] K. Park, W. J. Kim, Y. H. Cho et al., "Cancer gene therapy using adeno-associated virus vectors," *Frontiers in Bioscience*, vol. 13, no. 13, pp. 2653–2659, 2008.
- [16] H. Ameri, "Prospect of retinal gene therapy following commercialization of voretigene neparvovec-rzyl for retinal dystrophy mediated by RPE65 mutation," *Journal of Current Ophthalmology*, vol. 30, no. 1, pp. 1–2, 2018.
- [17] R. L. Kendall, G. Wang, and K. A. Thomas, "Identification of a natural soluble form of the vascular endothelial growth factor receptor, FLT-1, and its heterodimerization with KDR," *Biochemical and Biophysical Research Communications*, vol. 226, no. 2, pp. 324–328, 1996.
- [18] S. H. S. Lee, H. J. Kim, O. K. Shin et al., "Intravitreal injection of AAV expressing soluble VEGF receptor-1 variant induces anti-VEGF activity and suppresses choroidal neovascularization," *Investigative Ophthalmology & Visual Science*, vol. 59, no. 13, pp. 5398–5407, 2018.
- [19] B. L. Furman, "Streptozotocin-induced diabetic models in mice and rats," *Current Protocols in Pharmacology*, vol. 70, pp. 5–47, 2015.
- [20] J. C. Chou, S. D. Rollins, and A. A. Fawzi, "Trypsin digest protocol to analyze the retinal vasculature of a mouse model," *Journal of Visualized Experiments*, vol. 76, no. 76, article e50489, 2013.
- [21] U. C. S. Yadav, S. K. Srivastava, and K. V. Ramana, "Prevention of VEGF-induced growth and tube formation in human retinal endothelial cells by aldose reductase inhibition," *Journal of Diabetes and its Complications*, vol. 26, no. 5, pp. 369–377, 2012.
- [22] J. Lechner, O. E. O'Leary, and A. W. Stitt, "The pathology associated with diabetic retinopathy," *Vision Research*, vol. 139, pp. 7–14, 2017.
- [23] E. H. Sohn, H. W. van Dijk, C. Jiao et al., "Retinal neurodegeneration may precede microvascular changes characteristic of diabetic retinopathy in diabetes mellitus," *Proceedings of the National Academy of Sciences*, vol. 113, no. 19, pp. E2655–E2664, 2016.
- [24] R. S. Apte, D. S. Chen, and N. Ferrara, "VEGF in signaling and disease: beyond discovery and development," *Cell*, vol. 176, no. 6, pp. 1248–1264, 2019.
- [25] S. H. S. Lee, *Inhibiting the Mechanistic Target of Rapamycin (mTOR) via RNA Interference as a Novel Human Gene Therapeutic Strategy for the Treatment of Diabetic Retinopathy*, [Ph.D. thesis], University of Ulsan, 2021.

- [26] S. Roy, S. Amin, and S. Roy, "Retinal fibrosis in diabetic retinopathy," *Experimental Eye Research*, vol. 142, pp. 71–75, 2016.
- [27] U. Schmidt-Erfurth, J. Garcia-Arumi, F. Bandello et al., "Guidelines for the management of diabetic macular edema by the European Society of Retina Specialists (EURETINA)," *Ophthalmologica*, vol. 237, no. 4, pp. 185–222, 2017.
- [28] M. W. Stewart, "A review of ranibizumab for the treatment of diabetic retinopathy," *Ophthalmology and Therapy*, vol. 6, no. 1, pp. 33–47, 2017.
- [29] R. P. Singh, M. J. Elman, S. K. Singh, A. E. Fung, and I. Stoilov, "Advances in the treatment of diabetic retinopathy," *Journal of Diabetes and its Complications*, vol. 33, no. 12, article 107417, 2019.
- [30] C. H. Liu, Z. Wang, Y. Sun, and J. Chen, "Animal models of ocular angiogenesis: from development to pathologies," *The FASEB Journal*, vol. 31, no. 11, pp. 4665–4681, 2017.
- [31] R. Robinson, V. A. Barathi, S. S. Chaurasia, T. Y. Wong, and T. S. Kern, "Update on animal models of diabetic retinopathy: from molecular approaches to mice and higher mammals," *Disease Models & Mechanisms*, vol. 5, no. 4, pp. 444–456, 2012.
- [32] M. Whitehead, S. Wickremasinghe, A. Osborne, P. Van Wijngaarden, and K. R. Martin, "Diabetic retinopathy: a complex pathophysiology requiring novel therapeutic strategies," *Expert Opinion on Biological Therapy*, vol. 18, no. 12, pp. 1257–1270, 2018.
- [33] J. Wang, X. Xu, M. H. Elliott, M. Zhu, and Y. Z. Le, "Müller cell-derived VEGF is essential for diabetes-induced retinal inflammation and vascular leakage," *Diabetes*, vol. 59, no. 9, pp. 2297–2305, 2010.
- [34] T. A. Gardiner, D. B. Archer, T. M. Curtis, and A. W. Stitt, "Arteriolar involvement in the microvascular lesions of diabetic retinopathy: implications for pathogenesis," *Microcirculation*, vol. 14, no. 1, pp. 25–38, 2007.
- [35] A. J. Barber and B. Baccouche, "Neurodegeneration in diabetic retinopathy: potential for novel therapies," *Vision Research*, vol. 139, pp. 82–92, 2017.
- [36] X. X. Zeng, Y. K. Ng, and E. A. Ling, "Neuronal and microglial response in the retina of streptozotocin-induced diabetic rats," *Visual Neuroscience*, vol. 17, no. 3, pp. 463–471, 2000.